

Combining Quantum Mechanics Methods with Molecular Mechanics Methods in ONIOM

Thom Vreven,^{*,†,‡} K. Suzie Byun,[‡] István Komáromi,^{‡,§} Stefan Dapprich,[‡]
John A. Montgomery, Jr.,[†] Keiji Morokuma,^{*,‡} and Michael J. Frisch[†]

*Gaussian, Inc., 340 Quinnipiac Street, Building 40, Wallingford, Connecticut 06492,
and Cherry Emerson Center for Scientific Computation and Department of Chemistry,
Emory University, Atlanta, Georgia 30322*

Received November 26, 2005

Abstract: The purpose of this paper is 2-fold. First, we present several extensions to the ONIOM(QM:MM) scheme. In its original formulation, the electrostatic interaction between the regions is included at the classical level. Here we present the extension to electronic embedding. We show how the behavior of ONIOM with electronic embedding can be more stable than QM/MM with electronic embedding. We also investigate the link atom correction, which is implicit in ONIOM but not in QM/MM. Second, we demonstrate some of the practical aspects of ONIOM(QM:MM) calculations. Specifically, we show that the potential surface can be discontinuous when there is bond breaking and forming closer than three bonds from the MM region.

1. Introduction

Hybrid methods allow the combination of two or more computational techniques in one calculation and make it possible to investigate the chemistry of very large systems with high precision. The region of the system where the chemical process takes place, for example bond breaking or bond formation, is treated with an appropriately accurate method, while the remainder of the system is treated at a lower level. The most common class of hybrid methods is formed by the QM/MM methods, which combine a quantum mechanical (QM) method with a molecular mechanics (MM) method.^{1–4} The ONIOM (our Own N-layer Integrated molecular Orbital molecular Mechanics) scheme is more general in the sense that it can combine any number of molecular orbital methods as well as molecular mechanics methods.^{5–13} Hybrid methods in general have been the subject of a number of recent reviews.^{14–22}

A variety of QM/MM schemes have been reported in the literature. Although the main concepts are similar, the methods differ in a number of details. One major distinction is in the treatment of covalent interaction between the two regions. The resulting dangling bonds in the QM calculation need to be saturated, and the simplest approach is to use link atoms.^{2,23} These are usually hydrogen atoms but can, in principle, be any atom that mimics the part of the system that it substitutes. Link atoms are used in a large proportion of QM/MM implementations as well as our ONIOM scheme. The main alternative to link atoms is the use of frozen orbitals, which can through parametrization and use of *p* and *d* orbitals describe a more accurate charge density than link atoms.^{1,24–26} Although the few studies that directly compare link atom methods with frozen orbital methods show that both schemes perform well,^{25,27} it appears generally accepted that the latter can provide a better description of the boundary. However, due to the required parametrization of the frozen orbitals, they lack the flexibility and generality of link atoms. In our implementation we exclusively use link atoms because we consider generality one of the key aspects of our ONIOM scheme, and it is not feasible to parametrize frozen orbitals for every possible method combination. It must be noted that to some extent also the accuracy of link atoms can be improved by parametrization. The electrone-

* Corresponding author fax: 203 284 2520; e-mail: thom@gaussian.com.

[†] Gaussian, Inc.

[‡] Emory University.

[§] Current address: Thrombosis and Haemostasis Research Group of the Hungarian Academy of Sciences at the University of Debrecen, H-4032 Debrecen, Hungary.

gativity can be modified through the use of a shift operator²⁸ or, in the case of semiempirical QM methods, the parameters involving link atoms can be adjusted.²⁹ We have not included this limited parametrization in our current method but may do so in the future. Besides frozen orbitals and link atoms, several QM/MM methods use pseudopotentials to handle the covalent interactions between the QM and MM regions.^{30,31}

The second main difference between various QM/MM methods is the way the electrostatic interaction between the two layers is treated.³² In its simplest form, the interaction between the QM and MM region is completely described by MM style terms. This includes the electrostatic interaction, which is then evaluated as the interaction of the MM partial charges with partial (point) charges assigned to the atoms in the QM region. This approach is usually referred to as *classical* or *mechanical embedding*. In the second approach, the charge distribution of the MM region interacts with the actual charge distribution of the QM region. In this case, the partial charges from the MM region are included in the QM Hamiltonian, which provides a more accurate description of the electrostatic interaction and, in addition, allows the wave function to respond to the charge distribution of the MM region. This approach is referred to as *electronic embedding*. In the original version of ONIOM, the QM region and MM region interact via mechanical embedding.

In this paper we present several issues that are specifically related to QM/MM and QM/QM/MM methods within the ONIOM framework, where we focus on aspects that are different in most other QM/MM schemes. We will discuss partitioning restrictions that follow from the fact that the ONIOM energy expression is in the form of an extrapolation, which we refer to as the *cancellation problem*. Further, we discuss the placement of the link atoms in the MM model system calculation. Finally, we extended our methods to include electronic embedding. For a discussion of the geometry optimization methods in our package we refer to a separate series of papers.^{33–36} In the following sections we will first introduce the details of the ONIOM method. We will not provide a comprehensive overview of QM/MM methods but do present a ‘generic QM/MM method’ that contains all the components that we need for comparison to ONIOM. From here on we will use the term ONIOM to denote the combination of QM methods with MM methods in the ONIOM framework and QM/MM to denote the ‘generic QM/MM method’. The ONIOM scheme has been implemented in the Gaussian suite of programs.³⁷ Some of the developments, however, are only available in the private development version of the program,³⁸ and it must be noted that a first version of electronic embedding in ONIOM was independently implemented by István Komáromi.

Finally, we want to clarify some of the misconceptions about our methods that occasionally seem to arise.³⁹ The ONIOM method as it is currently implemented is the latest incarnation of a series of hybrid methods developed by Morokuma and co-workers. This series includes IMOMM (Integrated Molecular Orbital + Molecular Mechanics), which combines a Molecular Orbital (MO) method with a MM method, and IMOMO (Integrated Molecular Orbital + Molecular Orbital), which combines two MO methods into

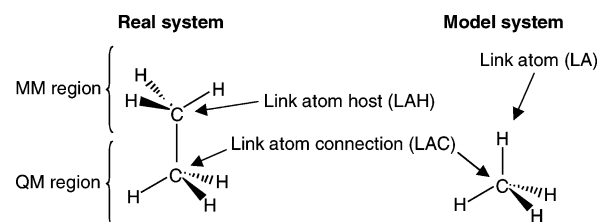


Figure 1. ONIOM terminology using ethane as an example.

one calculation. IMOMM and IMOMO are *not* a subset of ONIOM. The link atom position in ONIOM is obtained with a scale factor, while in IMOMM and IMOMO the link atom is placed at a specified distance from the atom to which it is connected. We consider the link atom treatment an intrinsic aspect of the ONIOM method.

2. Theory

2.1. MM Force Fields. An example of a typical force field, in this case Amber,⁴⁰ is of the form

$$E^{\text{total}} = \sum_{\text{bonds}} K_r (r - r_{\text{eq}})^2 + \sum_{\text{angles}} K_\theta (\theta - \theta_{\text{eq}})^2 + \sum_{\text{dihedrals}} \frac{V_n}{2} [1 + \cos(n\phi - \gamma)] + \sum_{i < j} \left[s_{ij}^{\text{vdw}} \left(\frac{A_{ij}}{r_{ij}^{12}} - \frac{B_{ij}}{r_{ij}^6} \right) + s_{ij}^q \frac{q_i q_j}{\epsilon r_{ij}} \right] \quad (1)$$

The first three terms describe the *bonded interactions*, formed by all the (chemical) bonds, angles, and dihedrals (including out-of-plane deformations) that are present in the system. The number of bonded terms scales linearly with the size of the system. The last term describes the *nonbonded interaction* between each pair of atom in the system. The van der Waals interaction, $(A_{ij}/r_{ij}^{12} - B_{ij}/r_{ij}^6)$, and the Coulomb interaction, $q_i q_j / \epsilon r_{ij}$, are scaled by factors s_{ij}^{vdw} and s_{ij}^q , respectively. The factors only differ from unity when the centers i and j are separated by three bonds or fewer, and the argument for using them is that the van der Waals and electrostatic interactions are already included in the bonded terms. The number of nonbonded terms scales quadratically with the size of the system and would be the bottleneck in MM calculations if computed as written in eq 1. Most implementations, however, use either distance based cutoffs or linear scaling methods for the evaluation of the nonbonded interaction. In our implementation we use cutoffs and a boxing algorithm to evaluate with the van der Waals interaction³⁵ and the Fast Multipole Method to deal with the electrostatic interaction.^{35,41–44}

2.2. ONIOM and QM/MM Energy Expressions. In a two-layer ONIOM(QM:MM) calculation, the total energy of the system is obtained from three independent calculations:

$$E^{\text{ONIOM}} = E^{\text{real,MM}} + E^{\text{model,QM}} - E^{\text{model,MM}} \quad (2)$$

The *real* system contains all the atoms and is calculated only at the MM level. The *model* system contains the part of the system that is treated at the QM level. Both QM and MM calculations need to be carried out for the model system. In Figure 1 we illustrate the terminology using ethane, where we include one methyl group in the QM region and the

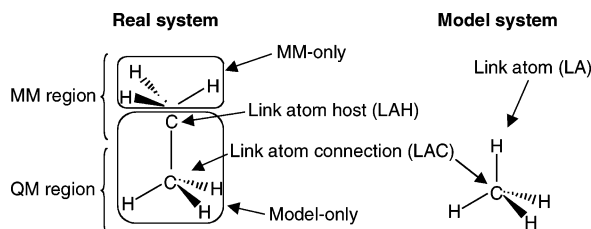


Figure 2. QM/MM terminology using ethane as an example.

remainder in the MM region. Because there is bonded interaction between the two regions, the model system includes a hydrogen link atom to saturate the open valence. The atoms that occur in both the model system and the real system have identical geometrical coordinates. The link atom (LA) is placed on the line that connects the center to which it is connected (the *Link Atom Connection*, LAC) with the atom that it substitutes (the *Link Atom Host*, LAH). The LAC-LA distance is obtained by scaling the original LAC-LAH distance with a constant factor, g , which is chosen so that a (chemically) reasonable LAC-LAH distance yields a reasonable LAC-LA distance.⁵

$$\mathbf{q}_{\text{LA}} = \mathbf{q}_{\text{LAC}} + g(\mathbf{q}_{\text{LAH}} - \mathbf{q}_{\text{LAC}}) \quad (3)$$

We will now relate the ONIOM(QM:MM) expression to the generic QM/MM scheme. The latter can be written as

$$E^{\text{QM/MM}} = E^{\text{MM-only,MM}} + E^{\text{model,QM}} + E^{\text{MM-only*model-only,MM}} \quad (4)$$

In Figure 2 we illustrate the QM/MM terminology. We assume that the position of the link atom is the same as in the ONIOM scheme. $E^{\text{MM-only,MM}}$ is the MM energy of the part of the system that only involves MM atoms (thus excluding the LA's). $E^{\text{MM-only*model-only,MM}}$ describes the interaction between the QM region and the MM region and contains all the MM terms that have at least one center in the MM-only region and at least one center in the model-only region. The QM/MM equation reflects a different approach than the ONIOM equation: Equation 4 is a summation scheme. It adds the QM energy of the QM region, the MM energy of the MM region, and the MM interaction energies between the two regions. The ONIOM expression 2, on the other hand, is cast as an extrapolation scheme. Note that in the ONIOM expression all three subcalculations are on 'complete systems', whereas in the QM/MM expression two of the terms are on partial systems, which is the reason for only ONIOM allowing the combination of QM methods with QM methods.

In the ONIOM scheme, most of the MM terms in the model system exist in the real system as well and cancel exactly in the full expression. The difference between the real system and model system MM calculations, the S -value, describes the contribution from the MM region, which includes both the energy of the MM region as well as the interaction between the QM region and the MM region.

$$S^{\text{MM}} = E^{\text{real,MM}} - E^{\text{model,MM}} \quad (5)$$

S^{MM} plays the same roll as the $E^{\text{MM-only,MM}} +$

$E^{\text{MM-only*model-only,MM}}$ terms in the QM/MM expression. In fact, when no bonded interactions are present between the regions, S^{MM} is identical to $(E^{\text{MM-only,MM}} + E^{\text{MM-only*model-only,MM}})$, and also the ONIOM and QM/MM energies become identical.

When bonded interactions are present in the system, the ONIOM and QM/MM functions are not identical. The terms involving LA in the model system calculation are not identical to the terms involving LAH in the real system calculation and do not cancel. The difference between the terms describes the difference between the LA and the LAH and can be interpreted as the MM extrapolation (or correction) of the link atoms in the model system QM calculation to the corresponding LAH atoms in the real system. In the generic QM/MM scheme, this extrapolation (or any other way to correct the QM link atom) is not present, although several QM/MM methods deal with this issue in other ways.

It is clear that when the ONIOM scheme is applied in its original formalism, as in eq 2, the interaction between the QM and MM regions is included via the MM calculations and therefore follows the *mechanical embedding* formalism. For this reason we also presented the generic QM/MM method in its mechanical embedding form. Later we will present *electronic embedding* formalisms for both ONIOM and QM/MM.

2.3. Derivatives and Three-Layer ONIOM. Derivatives with respect to geometrical coordinates and other properties can be obtained with the ONIOM formalism.⁵ For example, the gradient is written as

$$\frac{E^{\text{ONIOM}}}{\partial \mathbf{q}} = \frac{E^{\text{real,MM}}}{\partial \mathbf{q}} + \frac{E^{\text{model,QM}}}{\partial \mathbf{q}_{\text{QM}}^{\text{M}}} \mathbf{J}_{\text{QM}} - \frac{E^{\text{model,MM}}}{\partial \mathbf{q}_{\text{MM}}^{\text{M}}} \mathbf{J}_{\text{MM}} \quad (6)$$

\mathbf{q} is a vector that contains the Cartesian coordinates of the real system, and $\mathbf{q}_{\text{QM}}^{\text{M}}$ and $\mathbf{q}_{\text{MM}}^{\text{M}}$ are the Cartesian coordinates of the QM and MM model systems, respectively. The Jacobian \mathbf{J} projects the gradients of the link atoms onto the link atom host (LAH) and connection (LAC) coordinates. Because the positions of the link atoms is a function of the geometry of the real system, there are no additional (or fewer) degrees of freedom in the ONIOM scheme, and the potential function is well-defined. ONIOM can therefore be used in standard geometry optimization schemes and almost every other technique for the investigation of potential energy surfaces.

In principle, ONIOM can handle any number of layers, although the current implementation is limited to three. This facilitates QM/QM/MM calculations, which can for a given accuracy handle much larger QM regions than regular QM/MM methods. The combined QM/QM region in ONIOM-(QM:QM:MM) is obtained in a similar manner as in ONIOM(QM:QM), using three independent QM subcalculations. This is conceptually different from the QM/QM/MM implementation using CDFT, in which only two QM subcalculations are carried out, and the wave functions are directly coupled.⁴⁵ The expression for ONIOM(QM-high:QM-low:MM), where QM-high and QM-low denote a high-

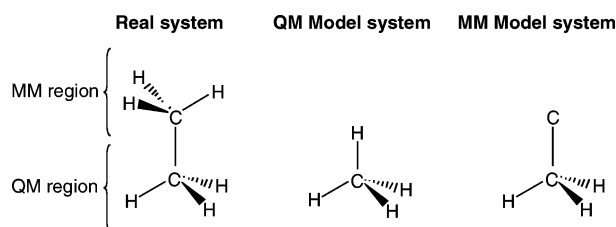


Figure 3. Alternative link atom placement in the MM model system in ONIOM.

Table 1: Vibrational Frequencies (cm^{-1}) of Ethane with ONIOM, B3LYP, and the Generic QM/MM

mode	B3LYP	QM/MM	ONIOM
$\text{CH}_3\text{--CH}_3$ twisting	312	317	316
asymmetric C–C–H bending (2)	832	903	972
C–C stretching	1010	786	955
symmetric C–C–H bending (2)	1235	1098	1168
asymmetric CH_3 umbrella	1433	1387	1468
symmetric CH_3 umbrella	1454	1474	1562
symmetric H–C–H bending (2)	1532	1414	1414
asymmetric H–C–H bending (2)	1537	1534	1549

level QM method and a low-level QM method, respectively, contains five terms:

$$E^{\text{ONIOM3}} = E^{\text{real,MM}} + E^{\text{intermediate,QM-low}} - E^{\text{intermediate,MM}} + E^{\text{model,QM-high}} - E^{\text{model,QM-low}} \quad (7)$$

Intermediate denotes the intermediate model system. Gradients and properties can be obtained for a three-layer system in the same way as for a two-layer system.

2.4. Link Atom Placement and Link Atom Extrapolation. When we first presented the ONIOM formalism, we assumed all the geometrical coordinates of the two model system calculations to be identical. The link atom scale factors are then the same for the QM and MM model systems, and also \mathbf{J}_{QM} and \mathbf{J}_{MM} in eq 6 are identical. In the most recent implementation we generalized the link atom placement and allow different scale factors g for the QM model system and the MM model system. The initial reason for lifting the restriction was to be able to minimize the error resulting from the link atom. In ONIOM(QM:MM) calculations, however, we can use this mechanism for a different purpose, which we illustrate in Figure 3. The QM model system calculation is obtained in the usual way with ‘chemically reasonable scale factors’, but the MM model system is obtained with unit scale factors, and \mathbf{J}_{MM} is a unit matrix. In addition, the MM atom type of the link atom is kept the same as the LAH in the real system. Carrying out an ONIOM(QM:MM) calculation in this way has the advantage that no MM parametrization for the link atoms is required and that therefore any system for which MM parameters are available can also be treated with ONIOM-(QM:MM). However, close inspection of the MM terms in the ONIOM energy expression shows that all the MM terms from the model system occur in the real system as well and therefore cancel. Since the terms involving LAH and LA are now identical, the extrapolation of the LA to the LAH is no longer present. In fact, the ONIOM(QM:MM) expression

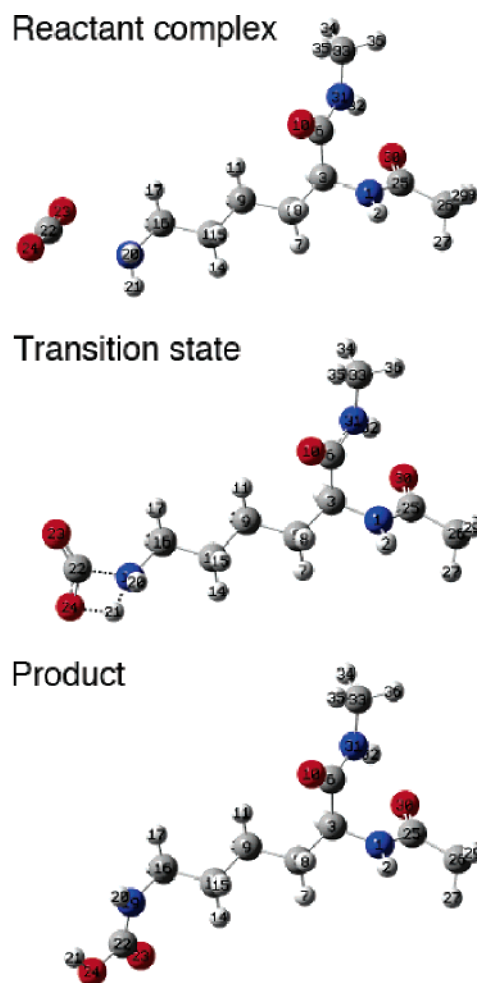


Figure 4. Carboxylation of lysine.

with unit scale factors for the MM model system becomes in this case identical to the QM/MM expression 4! Since the advantages of ONIOM(QM:MM) over QM/MM are removed with unit scale factors, we do not favor this.

The effect of the different link atoms placement is illustrated by the vibrational analysis of the ethane example from Figures 1–3. We calculated the vibrational spectrum at the B3LYP/6-31G(d) level of theory and compared this to the spectrum obtained with ONIOM and QM/MM. As outlined above, the latter is identical to ONIOM with the unit scale factor for the MM model system link atom. We used B3LYP/6-31G(d) for the QM method and the Amber force field for the MM method. In Table 1 we show the frequencies. The C–C stretching frequency is in bold. It is clear that the ONIOM value is much closer to the B3LYP reference value than the QM/MM value is. This is due to the link atom correction at the MM level of theory, which specifically improves the C–C stretch mode because it involves the border between the MM and QM region. Some of the other values are quite similar for QM/MM and ONIOM but differ significantly from B3LYP. These are modes that are either fully or partially located in the MM region and are therefore (partially) described by the MM parameters.

2.5. Cancellation Problem. We will now turn to a technical issue that needs to be taken into account when

Table 2: *S*-Values (Hartrees) for the Three Partitionings of the Carboxylation of Lysine

	reactant connectivity			product connectivity			$\Delta S(\text{TS})$
	$E^{\text{MM,Real}}(\text{TS})$	$E^{\text{MM,Model}}(\text{TS})$	$S(\text{TS,Reac})$	$E^{\text{MM,Real}}(\text{TS})$	$E^{\text{MM,Model}}(\text{TS})$	$S(\text{prod})$	
Partitioning 1							
Coulomb	-0.07858	-0.07807	-0.00051	-0.21806	-0.21072	-0.00735	0.00683
van der Waals	7.91222	7.89104	0.02118	0.10302	0.09556	0.00746	0.01372
stretching	0.06245	0.06144	0.00102	0.10449	0.10348	0.00102	0.00000
bending	0.01353	0.01008	0.00345	0.05744	0.05509	0.00235	0.00110
torsion	0.00825	0.00000	0.00825	0.00755	0.00000	0.00755	0.00070
out-of-plane	0.00002	0.00000	0.00002	0.00005	0.00004	0.00002	0.00000
total	7.91788	7.88448	0.03340	0.05449	0.04345	0.01105	0.02235
Partitioning 2							
Coulomb	-0.07858	-0.06837	-0.01021	-0.21806	-0.20726	-0.01080	0.00059
van der Waals	7.91222	7.90447	0.00775	0.10302	0.09522	0.00780	-0.00005
stretching	0.06245	0.06113	0.00132	0.10449	0.10317	0.00132	0.00000
bending	0.01353	0.01170	0.00183	0.05744	0.05562	0.00183	0.00000
torsion	0.00825	0.00076	0.00748	0.00755	0.00006	0.00748	0.00000
out-of-plane	0.00002	0.00000	0.00002	0.00005	0.00004	0.00002	0.00000
total	7.91788	7.90969	0.00819	0.05449	0.04685	0.00764	0.00054
Partitioning 3							
Coulomb	-0.07858	-0.06416	-0.01442	-0.21806	-0.20364	-0.01442	0.00000
van der Waals	7.91222	7.90432	0.00790	0.10302	0.09512	0.00790	0.00000
stretching	0.06245	0.06130	0.00115	0.10449	0.10334	0.00115	0.00000
bending	0.01353	0.01182	0.00171	0.05744	0.05574	0.00171	0.00000
torsion	0.00825	0.00077	0.00748	0.00755	0.00007	0.00748	0.00000
out-of-plane	0.00002	0.00000	0.00002	0.00005	0.00004	0.00002	0.00000
total	7.91788	7.91405	0.00383	0.05449	0.05066	0.00383	0.00000

studying chemical reactivity. Standard (nonreactive) MM methods cannot handle bond breaking and forming. As a general rule, relative energies only make sense when the structures are computed with the same atom types and connectivity. In other words, the potential function V needs to be continuous, which means that the list of angles, bends, etc. and the associated parameter cannot change. For example, consider the carboxylation of the lysine amino acid residue (Figure 4). The reactant and product have a different connectivity, and therefore the reaction energy cannot be computed with MM methods. Somewhere during the reaction (in the TS region), the connectivity changes from 'reactant' to 'product'. This introduces a discontinuity in the potential function, which is clearly wrong; for a method to describe bond breaking and forming correctly, the potential energy surface must be continuous.

In contrast to MM methods, ONIOM and QM/MM are able to describe bond breaking and forming. We illustrate this with the carboxylation example. The bond between H21 and O24 is broken in the reactant complex and formed in the product. In a MM calculation there is therefore a stretching term for this bond in the product but no stretching term in the complex. In a pure MM calculation, this results in a discontinuity in the potential surface. However, the ONIOM energy expression contains two MM terms, $E^{\text{real,MM}}$ and $E^{\text{model,MM}}$, and the stretching term for H21 and O24 occurs in both. Because these two H21–O24 stretching terms enter the energy expression with different sign, they cancel exactly and have no contribution to the ONIOM energy. The result is that the energy does not depend on whether the bond between H21 and O24 is considered being broken or formed

in the MM subcalculations. In other words, the ONIOM energy is continuous, despite the changes in the connectivity during the reaction.

We can present the issue raised in the previous paragraph in a more formal way. For the ONIOM surface to be continuous, the MM contribution to the energy must be continuous. The MM contribution is defined as the *S*-value, eq 5. Using the *S*-value, the ONIOM energy can be written as

$$E^{\text{ONIOM}} = E^{\text{model,QM}} + S^{\text{MM}} \quad (8)$$

For the *S*-value to be continuous, it must be independent of the definition of the connectivity in the reaction center. For example, when we take the transition state structure of the carboxylation reaction, the *S*-value calculated with the connectivity as in the reactant structure must be the same as the *S*-value calculated with the connectivity as in the product structure:

$$\Delta S^{\text{MM}} = S^{\text{MM}}(\text{TS,reactant connectivity}) - S^{\text{MM}}(\text{TS,product connectivity}) \Rightarrow \text{must be zero}$$

In Table 2 we show the S^{MM} and ΔS^{MM} values for the transition state of the carboxylation reaction, for the three partitionings in Figure 5. We calculated the *S*-value with both the reactant connectivity and the product connectivity and show the difference ΔS^{MM} in the final column. Besides the total MM values (in bold), we also show the values broken down for each type of MM term.

In the table we see that the reactant *S*-value and product *S*-value differ for both partitioning 1 and partitioning 2. Thus

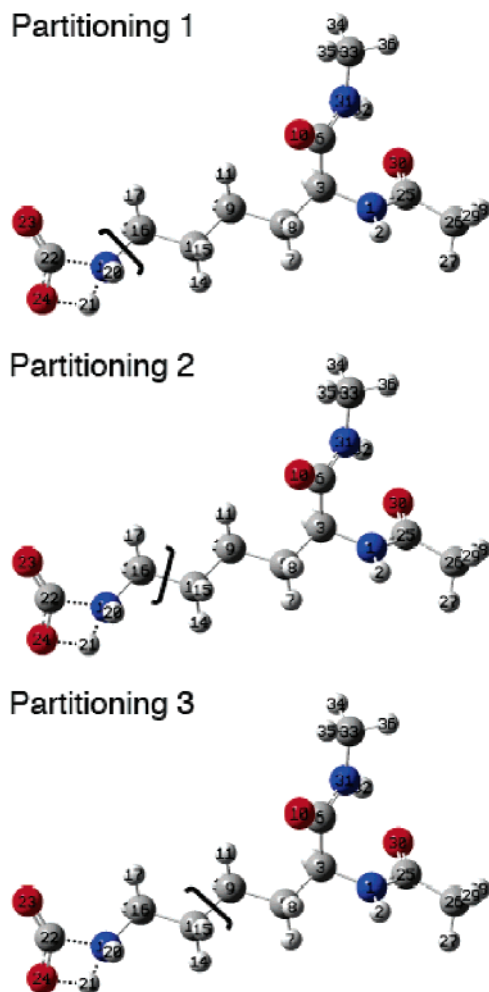


Figure 5. Partitionings for the carboxylation of lysine.

ΔS is not zero, and the result depends on the definition of the connectivity. This is clearly not what we expect from a correct partitioning, which we refer to as the *cancellation problem*.

How is it possible that ΔS is not zero, despite the only changes in the connectivity being completely in the QM region? From Table 2 we see that for partitioning 1, ΔS is zero for the stretching terms. Indeed, the stretching terms that are affected by the change in connectivity are identical and therefore cancel exactly in the real system and in the model system. However, the torsional terms, for example, have a nonzero ΔS for partitioning 1. Consider the torsional term for atoms H17–N19–H21–O24. This term does not exist in the model system, so its value does not cancel in the ONIOM expression. But whether this term is included in the energy expression (via the $E^{\text{MM,Real}}$ term) depends on whether the bond between N19 and H21 is considered broken or formed. If the bond is considered broken, the term will not enter the energy expression. If the bond is considered formed, it will enter the ONIOM energy expression. The result is that for partitioning 1, the total ONIOM energy depends on the connectivity and is not continuous. Therefore, partitioning 1 is wrong and should not be used. Looking at the table, partitioning 2 still produces a small energy difference, which results from the nonbonded terms that involve the link atom. This difference is so small that in

practice this partitioning can be used. Only the third partitioning generates exactly the same energies with both connectivity sets. Of course, this ‘cancellation problem’ is directly the result of MM terms extending over more than one bond. Since the ‘largest’ MM terms extend over three bonds (dihedral angle terms), the cancellation problem will never occur when there are more than three bonds between the MM region and any bond that is formed or broken during the reaction. However, avoiding the cancellation problem is only one requirement for a reliable potential. In most cases it will be necessary to include many more centers in the QM region in order to obtain meaningful results.

To summarize, when bond breaking and forming is part of the process in the QM region, it is safest to have the MM region at least three bonds away from the bond breaking/formation to avoid the cancellation problem. However, depending on the exact parameters involved in the MM terms in the border region, there are instances where one or two bond separations are sufficient. To test whether this is possible for a particular problem, one can apply the tests using the S -value as described in the paragraphs above. Although we discussed the problem with the cancellation using the ONIOM expression, it will occur with the generic QM/MM expression as well. The $E^{\text{MM-only*model-only,MM}}$ term in eq 4 contains all the MM terms that have at least one center in the MM-only region and at least one center in the model-only region. Again, which terms are included in $E^{\text{MM-only*model-only,MM}}$ depends on the connectivity, and the potential surface may be discontinuous when bond breaking and formation takes place close to the MM region.

2.6. Electronic Embedding. In QM/MM methods, there are two choices for dealing with the electrostatic interactions between the QM layer and the MM layer. The first, *classical embedding* or *mechanical embedding*, treats the cross-region electrostatic interactions at the molecular mechanics level. The second, *electronic embedding*, incorporates the cross-region electrostatic interaction in the QM Hamiltonian. The latter avoids the approximation of the QM charge distribution by point charges and allows the wave function to be polarized by the charge distribution of the MM region. From the original formulation, as outlined in the previous sections, it follows that ONIOM uses mechanical embedding by default. In this section we will present the modification of the ONIOM scheme to include electronic embedding. We also present the electronic embedding version of the generic QM/MM method and compare the two schemes in the results section.

To illustrate the different embedding approaches, we use the deprotonation of Histidine in Figure 6 as an example. The ONIOM expression contains two molecular mechanics terms, of which $E^{\text{model,MM}}$ includes the electrostatic interaction for the QM region, while $E^{\text{real,MM}}$ includes the electrostatic interaction for the *full* system. The latter includes the electrostatic interactions between atoms within the MM region, atoms within the QM region, and atoms in the QM region with atoms in the MM region. Electrostatic interactions between atoms that are separated by three bonds or less are scaled according to the MM force field definition, because they are (partially) implicit in the stretch, bend, and

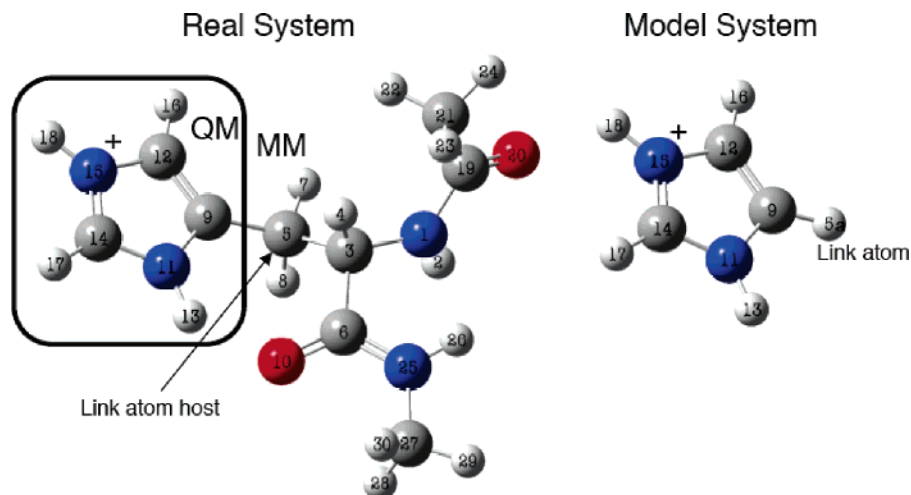


Figure 6. Real system, QM/MM partitioning, and model system for the (H18) deprotonation of histidine.

Table 3: Inclusion of Specific Interactions in the Standard (Mechanical Embedding) ONIOM(QM:MM) Energy Expression

centers	included in MM model system?	included in MM real system?	in QM model?
N1–C6	no (centers not in model)	no (2 bond separation)	no
N1–N25	no (centers not in model)	scaled (3 bond separation)	no
N1–C27	no (centers not in model)	yes	no
C3–C9	no (C3 not in model)	no (2 bond separation)	no
C3–C12	no (C3 not in model)	scaled (3 bond separation)	no
C3–N15	no (C3 not in model)	yes	no
C6–C9	no (C6 not in model)	scaled (3 bond separation)	no
C6–N11	no (C6 not in model)	yes	no
C6–C14	no (C6 not in model)	yes	no
C6–H17	no (C6 not in model)	yes	no
H16–C9	no (2 bond separation)	no (2 bond separation)	yes
H16–N11	scaled (3 bond separation)	scaled (3 bond separation)	yes
H16–H13	yes	yes	yes
C5–N11	no (C5 not in model system)	no (2 bond separation)	no
C5–C14	no (C5 not in model system)	scaled (3 bond separation)	no
C5–H17	no (C5 not in model system)	yes	no
H5a–N11	no (2 bond separation)	no (H5a not in real system)	yes
H5a–C14	scaled (3 bond separation)	no (H5a not in real system)	yes
H5a–H17	yes	no (H5a not in real system)	yes

torsional terms (For example, Amber uses a factor of zero for one and two bond separated electrostatic interactions and a factor of 1/1.2 for three bond separated interactions.). Using Figure 6, we show in Table 3 a number of specific interactions to illustrate which terms are included.

Because the interactions between QM and QM atoms (for example between H16 and H13) are included in *both* the $E_{\text{model,MM}}$ and the $E_{\text{real,MM}}$ terms, they cancel in the ONIOM energy expression. It follows that the only electrostatic interactions at the MM level that are retained in eq 1 are those between MM atoms and MM atoms and those between MM atoms and QM atoms. Hence, the electrostatic interaction between the two layers is described by the MM component of the energy expression, which is referred to as mechanical embedding. The point-charge electrostatic interactions involving LA and LAH are a special case. The interactions of the QM atoms with both LAH (C5) and LA (H5a) are retained but with different value, sign, and position. Their difference represents the extrapolation of the hydrogen link atom in the QM calculation to the carbon atom as it is

in the real system, similar to the bonded terms involving LA and LAH as discussed in the previous sections.

We will first discuss how the generic QM/MM scheme is extended to electronic embedding. The QM/MM energy expression 4 is modified to

$$E_{\text{QM/MM-EE}}^{\text{QM/MM-EE}} = E_{\text{MM-only,MM}}^{\text{MM-only,MM}} + E_{\text{v}}^{\text{model,QM}} + E_{\text{noQ}}^{\text{MM-only*model-only,MM}} \quad (9)$$

where

$$\hat{H}_{\text{v}}^{\text{model,QM}} = \hat{H}^{\text{model,QM}} - \sum_i \sum_N \frac{s_N q_N}{r_{iN}} + \sum_J \sum_N \frac{Z_J s_N q_N}{r_{JN}} \quad (10)$$

N , J , and i refer to the atoms from the MM region, atoms from the QM region, and electrons, respectively. The subscript noQ indicates that the electrostatic terms are excluded. The scaling factor s_N is used to avoid overpolarization of the wave function due to large charges close to the QM region. Usually s_N is zero for charges less than three

Table 4: Inclusion of Specific Interactions in the Generic Electronic Embedding QM/MM Energy Expression, with the Charges on C3 and C5 Scaled to Zero in the Model System Calculations^a

centers	included in MM model system?	included in MM real system?	in QM model?
N1–C6	no (centers not in model)	no (2 bond separation)	no
N1–N25	no (centers not in model)	scaled (3 bond separation)	no
N1–C27	no (centers not in model)	yes	no
C3–C9	<i>no (C3 scaled to zero)</i>	<i>no (excluded)</i>	<i>no (C3 scaled)</i>
C3–C12	<i>no (C3 scaled to zero)</i>	<i>no (excluded)</i>	<i>no (C3 scaled)</i>
C3–N15	<i>no (C3 scaled to zero)</i>	<i>no (excluded)</i>	<i>no (C3 scaled)</i>
C6–C9	yes	<i>no (excluded)</i>	yes
C6–N11	yes	<i>no (excluded)</i>	yes
C6–C14	yes	<i>no (excluded)</i>	yes
C6–H17	yes	<i>no (excluded)</i>	yes
H16–C9	no (2 bond separation)	no (2 bond separation)	yes
H16–N11	scaled (3 bond separation)	scaled (3 bond separation)	yes
H16–H13	yes	yes	yes
C5–N11	<i>no (C5 scaled to zero)</i>	<i>no (excluded)</i>	<i>no (C5 scaled)</i>
C5–C14	<i>no (C5 scaled to zero)</i>	<i>no (excluded)</i>	<i>no (C5 scaled)</i>
C5–H17	<i>no (C5 scaled to zero)</i>	<i>no (excluded)</i>	<i>no (C5 scaled)</i>
H5a–N11	<i>no (excluded)</i>	no (H5a not in real system)	yes
H5a–C14	<i>no (excluded)</i>	no (H5a not in real system)	yes
H5a–H17	<i>no (excluded)</i>	no (H5a not in real system)	yes

^a Entries in italics are different from those in Table 3.

bonds away from the QM region, and unit for the remaining charges. The scaling factor also avoids ‘overcounting’. For example, for the C3–C5–C9 angle there are molecular mechanics bending (C3–C5–C9) and stretching terms (C3–C5 and C5–C9) in $E_{\text{noQ}}^{\text{MM-only}*\text{model-only,MM}}$ (see Table 4). The electrostatic and van der Waals interactions between these three centers are implicit in these bending and stretching terms and are therefore excluded from the list of nonbonded interactions in MM calculations. However, if the partial charge of C3 were included in the QM Hamiltonian, the electrostatic interaction of this center with the charge density of C9 would be fully included via the term $E_{\text{v}}^{\text{model,QM}}$. The electrostatic interaction would then be included twice: once through the C3–C5–C9 bending term and once through the inclusion of the charge on C3 in the Hamiltonian. We refer to this as ‘overcounting’, and scaling the charge on C3 to zero ensures that it does not take place. This solution, however, is not satisfactory, because scaling the charge on C3 to zero results in the exclusion of the electrostatic interaction of this center with all the other QM atoms (C14, N15, etc.). Since these interactions should in fact be included, we refer to this as ‘undercounting’. In short, standard QM/MM will always result in either undercounting or overcounting, which is ultimately the result of the incompatibility between the QM charge density and the MM atom centered charges.

Some QM/MM implementations deal with the overpolarization and overcounting problem by using delocalized charges instead of point charges,^{46,47} or by redistributing the charges close to the QM region.⁴⁸ For electronic embedding in ONIOM we follow an approach that differs from standard QM/MM schemes. Following the spirit of ONIOM, we perform the model system calculations on the same system, which includes the charges that come from the MM region. In the QM model system these point charges are then incorporated in the Hamiltonian, while in the MM model

system calculation they are evaluated at the classical level. Furthermore, only the model system calculations are modified, while the real system MM term remains identical to that in the ONIOM-ME (ONIOM-Mechanical Embedding) expression 1. The expression for ONIOM-EE (ONIOM-Electronic Embedding) becomes

$$E^{\text{ONIOM-EE}} = E_{\text{v}}^{\text{model,QM}} + E^{\text{real,MM}} - E_{\text{v}}^{\text{model,MM}} \quad (11)$$

where

$$E_{\text{v}}^{\text{model,MM}} = E^{\text{model,MM}} + \sum_J \sum_N \frac{q_J s_N q_N}{r_{JN}} \quad (12)$$

The QM calculation in eq 11 is identical to that in eq 9. Because the model systems must be identical, we use the same scale factor s_N in both the QM and the MM model system calculations.

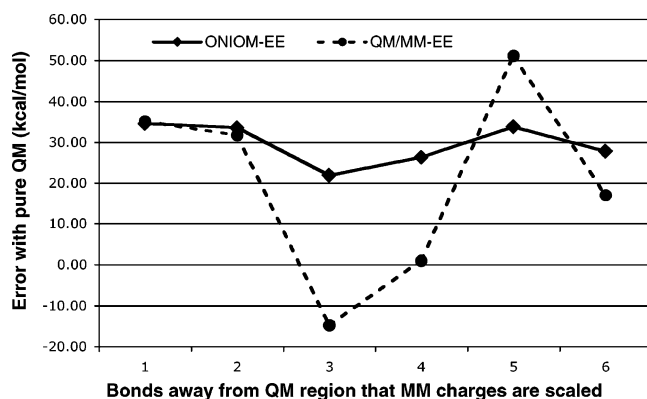
It must be noted that the use of delocalized or redistributed charges, as in other QM/MM schemes, is not mutually exclusive with the ONIOM implementation of electronic embedding. Applying both methods simultaneously might provide a superior scheme. Furthermore, from a practical point of view, a major difference between the QM/MM and ONIOM electronic embedding schemes is that in the latter the user must specify charges for the QM region.

In Table 5 we give again the specific electrostatic interactions in the MM terms, with the entries in italic being different from the corresponding Table 3 for ONIOM-ME. We will now compare the specific electrostatic interactions between standard QM/MM-EE and ONIOM-EE. With QM/MM-EE, we saw that the interaction between C3 and N15 is undercounted because the charge on C3 is scaled to zero in the QM calculation, and the C3–N15 interaction is excluded from the MM calculations. In the ONIOM-EE scheme, however, this interaction is still present in the $E^{\text{real,MM}}$

Table 5: Inclusion of Specific Interactions in the Electronic Embedding ONIOM(QM:MM) Energy Expression, with the Charges on C3 and C5 Scaled to Zero in the Model System Calculations^a

centers	included in MM model system?	included in MM real system?	in QM model?
N1–C6	no (centers not in model)	no (2 bond separation)	no
N1–N25	no (centers not in model)	scaled (3 bond separation)	no
N1–C27	no (centers not in model)	yes	no
C3–C9	<i>no (C3 scaled to zero)</i>	no (2 bond separation)	<i>no (C3 scaled)</i>
C3–C12	<i>no (C3 scaled to zero)</i>	scaled (3 bond separation)	<i>no (C3 scaled)</i>
C3–N15	<i>no (C3 scaled to zero)</i>	yes	<i>no (C3 scaled)</i>
C6–C9	yes	scaled (3 bond separation)	yes
C6–N11	yes	yes	yes
C6–C14	yes	yes	yes
C6–H17	yes	yes	yes
H16–C9	no (2 bond separation)	no (2 bond separation)	yes
H16–N11	scaled (3 bond separation)	scaled (3 bond separation)	yes
H16–H13	yes	yes	yes
C5–N11	<i>no (C5 scaled to zero)</i>	no (2 bond separation)	<i>no (C5 scaled)</i>
C5–C14	<i>no (C5 scaled to zero)</i>	scaled (3 bond separation)	<i>no (C5 scaled)</i>
C5–H17	<i>no (C5 scaled to zero)</i>	yes	<i>no (C5 scaled)</i>
H5a–N11	no (2 bond separation)	no (H5a not in real system)	yes
H5a–C14	scaled (3 bond separation)	no (H5a not in real system)	yes
H5a–H17	yes	no (H5a not in real system)	yes

^a Entries in italics are different from those in Table 3.

**Figure 7.** Error of ONIOM-EE and QM/MM-EE as a function of the charges scaled based on distance from the QM region.

term. The electrostatic interaction between C3 and N15 is therefore still included in the ONIOM expression, albeit at the classical level. Another example is the interaction between C6 and C9. The MM torsional term C9–C5–C3–C6 already contains implicitly part of the electrostatic interaction, which is why the three-bond separated non-bonded interactions are scaled. However, the C6–C9 electrostatic interaction is without scaling included in the QM term in equation $E_v^{\text{model,QM}}$. In QM/MM-EE this leads to overcounting, but in ONIOM-EE this particular interaction is included fully in the model system MM term $E_v^{\text{model,MM}}$ and scaled in the real system MM term $E^{\text{real,MM}}$. The difference between the MM terms can be regarded as a correction to the overcounting at the QM level. In other words, in ONIOM-EE the overcounting or undercounting introduced at the QM level is always corrected automatically at the classical level. This follows naturally from the ONIOM expressions and does not require any of the corrections that generic QM/MM-EE schemes need.

In Figure 7 we show the error of the ONIOM-EE and QM/MM-EE calculations on the deprotonation of histidine,

compared to full QM calculations. Our focus is not on the absolute performance of the hybrid schemes but rather on the difference in behavior between ONIOM and the generic QM/MM method. The graph shows the error as a function of the number of bonds away from the QM region that have the charges scaled to zero. The charge on C5 is always scaled to zero. At $x = 1$, only charges one bond out (C5) are scaled. At $x = 2$, charges up to two bonds out (C5, H7, H8, and C3) are scaled, and so forth.

Even though the QM/MM-EE has the smallest absolute error (at $x=4$), its behavior is much more erratic than ONIOM-EE. The reason is that, in this particular example, the sign of the charges in the MM region is alternating with each step further away from the QM region and that therefore the total charge included in the set of (nonzero) point charges changes strongly with each increasing x -value. In ONIOM-EE the total charge is always the same, because the error at the QM level is corrected at the MM level, and the graph is much less erratic.

At $x = 6$, all the charges in the MM region are scaled to zero in the model system calculations, and ONIOM-EE becomes identical to ONIOM-ME. We see that the result is quite similar to the ONIOM-EE results, which indicates that the partial charges assigned to the QM region describe the real QM charge density quite well. Note that ONIOM-EE and QM/MM-EE are not identical to each other when all the charges are scaled to zero, at $x = 6$. In that case, QM/MM-EE completely ignores all the electrostatic interactions between the two layers, while QM/MM-EE becomes ONIOM-ME and still includes the electrostatic interactions at the classical level, through the $E^{\text{real,MM}}$ calculation.

Finally, we want to stress that the example above is intended primarily to demonstrate that correct charge balancing follows naturally from the electronic embedding version of ONIOM. Our generic QM/MM implementation is crude in many ways, and the unfavorable comparison to ONIOM-

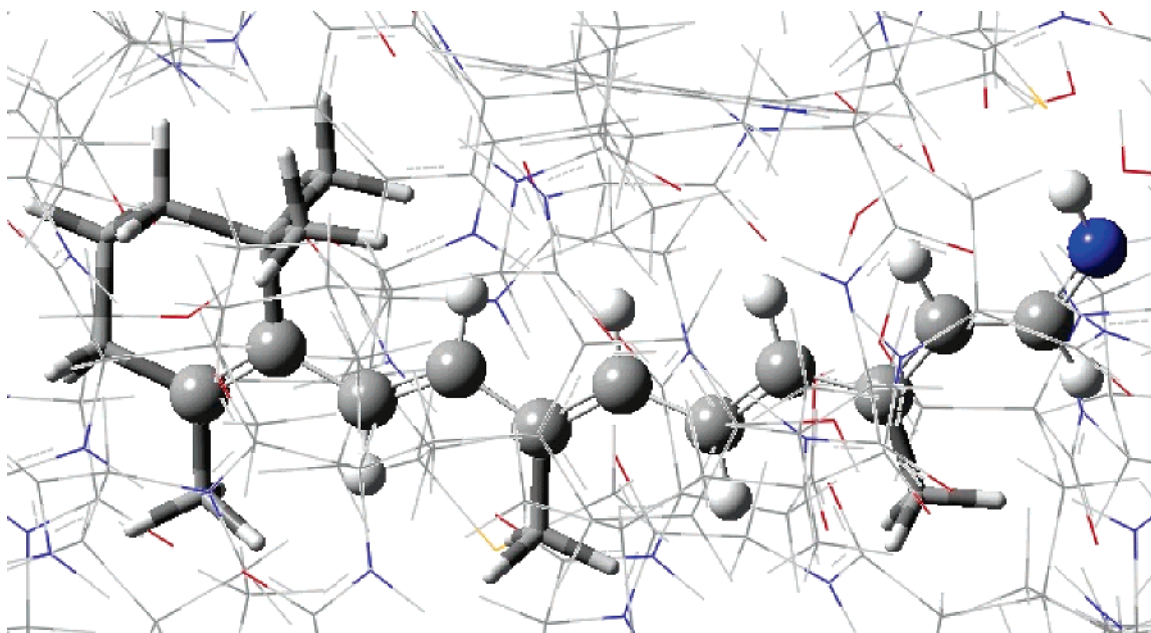


Figure 8. ONIOM3 partitioning of bR. Ball and stick represents B3LYP, tube HF, and wireframe the Amber molecular mechanics force field.

Table 6: Excitation Energies of BR for Various Partitionings and Method Combinations

	real (kcal/mol)	model-high (kcal/mol)	model-low (kcal/mol)	ONIOM (kcal/mol)	time (min)
HF:Amber-EE	81.45			81.45	39
B3:Amber-EE (benchmark)	58.25			58.25	318
B3:HF:Amber-EE	69.70	62.80	71.24	61.26	109
B3:HF:Amber-EEEx	72.33	60.78	69.62	63.50	102

EE in Figure 7 is not typical for state-of-the-art QM/MM implementations, which have incorporated other methods for dealing with the charge-balancing. These methods, however, are complimentary with ONIOM, and using both approaches simultaneously may provide the superior QM/MM scheme.

2.7. Three-Layer Electronic Embedding. In ONIOM-(QM-high:QM-low:MM)-EE, we need to decide which charges need to be included in each of the four QM model system calculations. In the calculations on the intermediate model system, we always include the MM charge density. In the calculation on the small model system, we have two choices. First, we can carry out the calculations on the small model system with the same charge cloud as the intermediate model system calculations. We denote this as ONIOM3-EE. Note that in this case, only the partial charges of the MM layer are included and not the charges associated with the intermediate layer. Second, we can carry out the calculations on the small model system without any charges, assuming that the effect of the charge cloud is accurately included via the calculations on the intermediate model system. This is denoted as ONIOM3-EEEx.

$$E^{\text{ONIOM3-EE}} = E_{\text{v}}^{\text{model,QM-high}} + E_{\text{v}}^{\text{intermediate,QM-low}} - E_{\text{v}}^{\text{model,QM-low}} + E^{\text{real,MM}} - E_{\text{v}}^{\text{intermediate,MM}} \quad (13)$$

$$E^{\text{ONIOM3-EEEx}} = E_{\text{v}}^{\text{model,QM-high}} + E_{\text{v}}^{\text{intermediate,QM-low}} - E_{\text{v}}^{\text{model,QM-low}} + E^{\text{real,MM}} - E_{\text{v}}^{\text{intermediate,MM}} \quad (14)$$

It depends on the problem whether ONIOM3-EE or ONIOM3-EEEx is the best choice. The QM-high layer can

be far away from the MM layer (with the QM-low layer acting as buffer). If the MM density is included in the model system calculations, following ONIOM3-EE, the QM-high layer ‘feels’ the full charge density. However, in reality the charges from the MM region will be screened by the QM-low layer. If this screening is important, ONIOM3-EE will be unphysical. Excluding the MM charges from the model system calculation, in ONIOM3-EEEx, is not always correct either, especially when the QM-low method cannot describe accurately the effect of the MM charge distribution on the QM-high layer.

To illustrate the three-layer version of ONIOM with electronic embedding, we use the $S_0 \rightarrow S_1$ excitation in bacteriorhodopsin (bR) from ref 11. We include the complete chromophore in the intermediate model system, while the chromophore without the substituents (only the Schiff base polyene) is in the small model system (Figure 8). The levels of theory used are B3LYP/6-31G(d) for QM-high and HF/3-21G for QM-low and TD-B3LYP and TD-HF for the excitation energies. We calculated the HF:Amber and B3LYP:HF:Amber excitations on the geometries optimized at the specific level of theory.

In Table 6 we show the excitation energies for the three-layer ONIOM calculations as well as two-layer ONIOM calculations. In the latter, the full chromophore is included in the QM region. The two-layer B3LYP:Amber calculation then forms the benchmark to which we compare the results.

The results are clear. B3LYP:HF:Amber does always a better job than the two-layer HF:Amber. In addition, for this example it does appear necessary to include the charge cloud also in the smallest model system, although the difference is small. In the three-layer calculation, we obtain virtually identical results, for about a third of the CPU time as needed in the two-layer calculation.

3. Conclusions

We presented several developments of the ONIOM(QM:MM) method and compared the behavior and performance to a generic QM/MM scheme. The electronic embedding version of ONIOM appears to be more stable than QM/MM with electronic embedding. However, we implemented only the simple charge zeroing version of the latter, and QM/MM might compare more favorably to ONIOM when more sophisticated methods for avoiding overpolarization are implemented, such as delocalized charges or charge redistribution. Combining these methods with the ONIOM scheme may present a superior scheme for electronic embedding. Furthermore, we showed that the link atom correction that is implicit in ONIOM and omitted from simple QM/MM schemes can improve the results significantly.

We analyzed in detail the occurrence of discontinuities in the ONIOM(QM:MM) energy when bond breaking and formation is involved. The 'better safe than sorry' approach is to ensure that there are at least three bonds between the MM region and the bonds in the QM region that are being broken or formed. In some cases it may be possible to have only one or two bonds, but careful testing is required to ensure that the potential is correct.

To conclude, we feel that the extrapolation nature of ONIOM provides elegant and implicit solutions to some problems, especially related to charge balancing, that require ad-hoc corrections in most other QM/MM schemes. Some of the solutions that follow from the ONIOM method can be incorporated in other QM/MM schemes. In turn, many of the promising developments in other QM/MM methods can be formulated in the ONIOM framework as well.

Acknowledgment. K.M. acknowledges support in part by a grant (CHE-0209660) from the U.S. National Science Foundation and by a grant from Gaussian, Inc.

References

- (1) Warshel, A.; Levitt, M. *J. Mol. Biol.* **1976**, *103*, 227–249.
- (2) Maseras, F.; Morokuma, K. *J. Comput. Chem.* **1995**, *16*, 1170–1179.
- (3) Field, M. J.; Bash, P. A.; Karplus, M. *J. Comput. Chem.* **1990**, *11*, 700–733.
- (4) Singh, U. C.; Kollman, P. A. *J. Comput. Chem.* **1986**, *7*, 718–730.
- (5) Dapprich, S.; Komáromi, I.; Byun, K. S.; Morokuma, K.; Frisch, M. J. *J. Mol. Struct. (THEOCHEM)* **1999**, *461–462*, 1–21.
- (6) Svensson, M.; Humbel, S.; Froese, R. D. J.; Matsubara, T.; Sieber, S.; Morokuma, K. *J. Phys. Chem.* **1996**, *100*, 19357–19363.
- (7) Vreven, T.; Mennucci, B.; da Silva, C. O.; Morokuma, K.; Tomasi, J. *J. Chem. Phys.* **2001**, *115*, 62–72.
- (8) Karadakov, P. B.; Morokuma, K. *Chem. Phys. Lett.* **2000**, *317*, 589–596.
- (9) Rega, N.; Iyengar, S. S.; Voth, G. A.; Schlegel, H. B.; Vreven, T.; Frisch, M. J. *J. Phys. Chem. B* **2004**, *108*, 4210–4220.
- (10) Humbel, S.; Sieber, S.; Morokuma, K. *J. Chem. Phys.* **1996**, *105*, 1959–1967.
- (11) Vreven, T.; Morokuma, K. *Theor. Chem. Acc.* **2003**, *109*, 125–132.
- (12) Vreven, T.; Morokuma, K. *J. Comput. Chem.* **2000**, *21*, 1419–1432.
- (13) Hopkins, B. W.; Tschumper, G. S. *J. Comput. Chem.* **2003**, *24*, 1563.
- (14) Warshel, A. *Annu. Rev. Biophys. Biomol. Struct.* **2003**, *32*, 425–443.
- (15) Ujaque, G.; Maseras, F. *Structure Bonding* **2004**, *112*, 117–149.
- (16) Gao, J. In *Reviews in Computational Chemistry*; Lipkowitz, K. B., Boyd, D. B., Eds.; VCH Publishers: New York, 1996; Vol. 7, pp 119–301.
- (17) Froese, R. D. J.; Morokuma, K. In *Encyclopedia of Computational Chemistry*; Schleyer, P. v. R., Allinger, N. L., Kollman, P. A., Clark, T., Schaefer, H. F., III, Gasteiger, J., Schreiner, P. R., Eds.; Wiley: Chichester, 1998; Vol. 2, pp 1244–1257.
- (18) Gao, J. In *Encyclopedia of Computational Chemistry*; Schleyer, P. v. R., Allinger, N. L., Kollman, P. A., Clark, T., Schaefer, H. F., III, Gasteiger, J., Schreiner, P. R., Eds.; Wiley: Chichester, 1998; Vol. 2, pp 1257–1263.
- (19) Merz, K. M.; Stanton, R. V. In *Encyclopedia of Computational Chemistry*; Schleyer, P. v. R., Allinger, N. L., Kollman, P. A., Clark, T., Schaefer, H. F., III, Gasteiger, J., Schreiner, P. R., Eds.; Wiley: Chichester, 1998; Vol. 4, pp 2330–2343.
- (20) Ruiz-López, M. F.; Rivail, J. L. In *Encyclopedia of Computational Chemistry*; Schleyer, P. v. R., Allinger, N. L., Kollman, P. A., Clark, T., Schaefer, H. F., III, Gasteiger, J., Schreiner, P. R., Eds.; Wiley: Chichester, 1998; Vol. 1.
- (21) Tomasi, J.; Pomelli, C. S. In *Encyclopedia of Computational Chemistry*; Schleyer, P. v. R., Allinger, N. L., Kollman, P. A., Clark, T., Schaefer, H. F., III, Gasteiger, J., Schreiner, P. R., Eds.; Wiley: Chichester, 1998; Vol. 4, pp 2343–2350.
- (22) Vreven, T.; Morokuma, K. *Ann. Rep. Comput. Chem.*, in press.
- (23) Derat, E.; Bouquant, J.; Humbel, S. *J. Mol. Struct. (THEOCHEM)* **2003**, *632*, 61–69.
- (24) Thery, V.; Rinaldi, D.; Rivail, J. L.; Maigret, B.; Ferenczy, G. G. *J. Comput. Chem.* **1994**, *15*, 269–282.
- (25) Reuter, N.; Dejaegere, A.; Maigret, B.; Karplus, M. *J. Phys. Chem. A* **2000**, *104*, 1720–1735.
- (26) Gao, J.; Amara, P.; Alhambra, C.; Field, M. J. *J. Phys. Chem. A* **1998**, *102*, 4714–4721.
- (27) Nicoll, R. M.; Hindle, S. A.; MacKenzie, G.; Hillier, I. H.; Burton, N. A. *Theor. Chem. Acc.* **2000**, *106*, 105–112.
- (28) Koga, N.; Morokuma, K. *Chem. Phys. Lett.* **1990**, *172*, 243–248.

- (29) Antes, I.; Thiel, W. *J. Phys. Chem. A* **1999**, *103*, 9290–9295.
- (30) Zhang, Y. K.; Lee, T. S.; Yang, W. T. *J. Chem. Phys.* **1999**, *110*, 46–54.
- (31) DiLabio, G. A.; Hurley, M. M.; Christiansen, P. A. *J. Chem. Phys.* **2002**, *116*, 9578–9584.
- (32) Bakowies, D.; Thiel, W. *J. Phys. Chem.* **1996**, *100*, 10580–10594.
- (33) Vreven, T. Manuscript in preparation.
- (34) Vreven, T. Manuscript in preparation.
- (35) Vreven, T.; Frisch, M. J.; Kudin, K. N.; Schlegel, H. B.; Morokuma, K. *Mol. Phys.* **2006**, *104*, 701–714.
- (36) Vreven, T.; Morokuma, K.; Farkas, Ö.; Schlegel, H. B.; Frisch, M. J. *J. Comput. Chem.* **2003**, *24*, 760–769.
- (37) Frisch, M. J.; Trucks, G. W.; Schlegel, H. B.; Scuseria, G. E.; Robb, M. A.; Cheeseman, J. R.; Montgomery, J. A., Jr.; Vreven, T.; Kudin, K. N.; Burant, J. C.; Millam, J. M.; Iyengar, S. S.; Tomasi, J.; Barone, V.; Mennucci, B.; Cossi, M.; Scalmani, G.; Rega, N.; Petersson, G. A.; Nakatsuji, H.; Hada, M.; Ehara, M.; Toyota, K.; Fukuda, R.; Hasegawa, J.; Ishida, M.; Nakajima, T.; Honda, Y.; Kitao, O.; Nakai, H.; Klene, M.; Li, X.; Knox, J. E.; Hratchian, H. P.; Cross, J. B.; Adamo, C.; Jaramillo, J.; Gomperts, R.; Stratmann, R. E.; Yazyev, O.; Austin, A. J.; Cammi, R.; Pomelli, C.; Ochterski, J. W.; Ayala, P. Y.; Morokuma, K.; Voth, G. A.; Salvador, P.; Dannenberg, J. J.; Zakrzewski, V. G.; Dapprich, S.; Daniels, A. D.; Strain, M. C.; Farkas, O.; Malick, D. K.; Rabuck, A. D.; Raghavachari, K.; Foresman, J. B.; Ortiz, J. V.; Cui, Q.; Baboul, A. G.; Clifford, S.; Cioslowski, J.; Stefanov, B. B.; Liu, G.; Liashenko, A.; Piskorz, P.; Komaromi, I.; Martin, R. L.; Fox, D. J.; Keith, T.; Al-Laham, M. A.; Peng, C. Y.; Nanayakkara, A.; Challacombe, M.; Gill, P. M. W.; Johnson, B.; Chen, W.; Wong, M. W.; Gonzalez, C.; Pople, J. A. *Gaussian 03 Revision C.02 ed.*; Gaussian, Inc.: Wallingford, CT, 2004.
- (38) Frisch, M. J.; Trucks, G. W.; Schlegel, H. B.; Scuseria, G. E.; Robb, M. A.; Cheeseman, J. R.; Montgomery, J. A., Jr.; Vreven, T.; Kudin, K. N.; Burant, J. C.; Millam, J. M.; Iyengar, S. S.; Tomasi, J.; Barone, V.; Mennucci, B.; Cossi, M.; Scalmani, G.; Rega, N.; Petersson, G. A.; Nakatsuji, H.; Hada, M.; Ehara, M.; Toyota, K.; Fukuda, R.; Hasegawa, J.; Ishida, M.; Nakajima, T.; Honda, Y.; Kitao, O.; Nakai, H.; Klene, M.; Li, X.; Knox, J. E.; Hratchian, H. P.; Cross, J. B.; Adamo, C.; Jaramillo, J.; Gomperts, R.; Stratmann, R. E.; Yazyev, O.; Austin, A. J.; Cammi, R.; Pomelli, C.; Ochterski, J. W.; Ayala, P. Y.; Morokuma, K.; Voth, G. A.; Salvador, P.; Dannenberg, J. J.; Zakrzewski, V. G.; Dapprich, S.; Daniels, A. D.; Strain, M. C.; Farkas, O.; Malick, D. K.; Rabuck, A. D.; Raghavachari, K.; Foresman, J. B.; Ortiz, J. V.; Cui, Q.; Baboul, A. G.; Clifford, S.; Cioslowski, J.; Stefanov, B. B.; Liu, G.; Liashenko, A.; Piskorz, P.; Komaromi, I.; Martin, R. L.; Fox, D. J.; Keith, T.; Al-Laham, M. A.; Peng, C. Y.; Nanayakkara, A.; Challacombe, M.; Gill, P. M. W.; Johnson, B.; Chen, W.; Wong, M. W.; Gonzalez, C.; Pople, J. A. *Gaussian 03 Revision C.01 ed.*; Gaussian, Inc.: Wallingford, CT, 2004.
- (39) Swart, M. *Int. J. Quantum Chem.* **2002**, *91*, 177–183.
- (40) Cornell, W. D.; Cieplak, P.; Bayly, C. I.; Gould, I. R.; Merz, K. M.; Ferguson, D. M.; Spellmeyer, D. C.; Fox, T.; Caldwell, J. W.; Kollman, P. A. *J. Am. Chem. Soc.* **1995**, *117*, 5179.
- (41) Kudin, K. N.; Scuseria, G. E. *Chem. Phys. Lett.* **1998**, *283*, 61–68.
- (42) Strain, M. C.; Scuseria, G. E.; Frisch, M. J. *Science* **1996**, *271*, 51.
- (43) Greengard, L. *The rapid evaluation of potential fields in particle systems*; MIT Press: Cambridge, MA, 1988.
- (44) Greengard, L.; Rokhlin, V. *J. Comput. Phys.* **1987**, *73*, 325.
- (45) Strajbl, M.; Hong, G.; Warshel, A. *J. Phys. Chem. B* **2002**, *106*, 13333–13343.
- (46) Amara, P.; Field, M. J. *Theor. Chem. Acc.* **2003**, *109*, 43–52.
- (47) Das, D.; Eurenus, K. P.; Billings, E. M.; Sherwood, P.; Chatfield, D. C.; Hodoscek, M.; Brooks, B. R. *J. Chem. Phys.* **2002**, *117*, 10534–10547.
- (48) Lin, H.; Trulahr, D. G. *J. Phys. Chem. A* **2005**, *109*, 3991–4004.

CT050289G